polymer

Strain-induced crystallization of natural rubber as detected real-time by wide-angle X-ray diffraction technique

S. Toki[a,*], T. Fujimaki[b], M. Okuyama[b]

[a]*Polymer Engineering Institute, University of Akron, Akron, OH 44325-0301, USA*
[b]*Bridgestone Corporation, Kodairashi, Tokyo 187-8531, Japan*

Abstract

In the past, the stress–strain behavior of natural rubber has been studied by a variety of mechanical analytical techniques in order to understand the role of induced crystallization by deformation. But, this was generally done in a sequential manner by stretching to a certain extent and examining the stretched part separately. This type of sequential experiment may not follow the exact dynamics of the process and thus may lead to erroneous conclusions regarding the evolution of microscopic mechanisms. It is therefore advantageous to measure the mechanical response simultaneously with the structural response to map the structural evolution onto the stress–strain behavior. In this paper, simultaneous measurements of the stress–strain behavior and X-ray scattering intensity of vulcanized natural rubber were made continuously by a specially designed instrument during elongation and subsequent retraction. These studies revealed three new characteristics of the strain-induced crystallization. 1. The strain-induced crystallization starts at around 400% strain at 25°C, then increases steeply, although sequential measurements reported that natural rubber starts strain-induced crystallization at 200%. 2. At the onset of retracting, the degree of crystallinity continues to increase, although a drastic decrease of stress occurs. We suggest the morphology of the strain-induced crystallites changes such that do not contribute to stress. 3. Strain-induced crystallites disappear at the strain where the stress–strain loop is closed during retracting. The hysteresis of the stress–strain curve might be attributed to strain-induced crystallization. © 2000 Elsevier Science Ltd. All rights reserved.

Keywords: Strain; Crystallization; Wide-angle X-ray scattering

1. Introduction

Vulcanized natural rubber is known as an exceptionally tough elastomer because it exhibits high tensile stress, large hysteresis loss, and crystallization upon stretching. The strength of the natural rubber has been attributed to this strain-induced crystallizability. The crystallization of natural rubber in both the stretched and the unstretched condition at various temperatures has been studied extensively by many researchers [1–10]. The strain/stress induced and the temperature/time induced crystallization have been analyzed by volume-change measurements [1,3], stress relaxation [1,3,4], electron microscopy [5–12], birefringence [13–16], infrared absorption [17], X-ray diffraction [1,4,8–10,16,18] and pulsed NMR [19] techniques. It is observed that undeformed natural rubber forms spherulitic crystallites below 0°C [5–10]. The temperature/time induced crystallites generally form as folded chain

lamellae. The morphology of the strain/stress induced crystallites has been reported to have various; fibrils, fibrils and folded lamellae, and shish-kebabs [2,4–10,15]. The degree of crystallinity and the stress–strain relation have been compared using birefringence, X-ray diffraction, pulsed NMR and IR. But almost all of these experiments were done with sequential measurements in which first the sample is extended to a desired strain and fixed at that strain, and then the sample is removed from the stretching instrument. Finally the sample is fixed on the analyzing instrument and examined. Most of those who made measurements in a sequential manner intended to avoid any non-equilibrium effects associated with the original stretching [8–10].

For the stress–strain measurements, the sample was stretched and allowed to retract continuously. In order to understand what occurred during stretching and during retraction, we have to examine the sample simultaneously with the strain. Both sequential and simultaneous measurements of stress–strain and birefringence have been made [1,13,15]. These authors have shown that the birefringence during retraction is more than that developed during

* Corresponding author. Tel.: +1-330-972-5736; fax: +1-330-258-2339.
 E-mail address: toki@poly-eng.uakron.edu (S. Toki).

Table 1
Poly-isoprene samples used in this study (a grade of NR(Hevia) is RSS-4 (RSS = Ribbed Smoked Sheet))

Polymer	Supplier	%cis-1,4	$M_n \times 10^{-5}$	M_w/M_n
NR		100	2.3	6.00
IR2000	JSR	98	6.1	3.13
Cariflex 309	Shell	91	4.8	3.02

stretching, but the stress during retraction is less than that developed during stretching. This indicates that a substantial portion of the total orientation of the amorphous and crystalline regions is delayed until the retraction stage, suggesting a complex crystallization orientation mechanism. The induced crystalline order itself can be analyzed directly by wide-angle X-ray techniques. X-ray diffraction analyses on natural rubber have been done in a sequential manner [4,8–10,16,18]. They have shown that strain-induced crystallization occurs at a relatively low strain, such as 200%, then gradually increases. Several hours were required to examine the samples at each strain.

In the present paper, we will show the dynamic process of strain-induced crystallization by simultaneously measuring the X-ray scattering intensity–strain and stress–strain behavior.

2. Experimental procedures

2.1. Materials

Natural rubber (Hevea) was chosen. Synthetic poly-isoprenes (JSR IR-2200 and Shell Cariflex-309) were selected as references. The chemical structures and molecular weights are summarized in Table 1. The polymers were compounded with various ingredients in a Brabender mixer. The recipes of the compounds are shown in Table 2. The compounds were cured into $2 \times 15 \times 15$ mm sheets at 140°C for 30 min. Ring-shaped samples were cut from the sheet, with outer diameter 27 mm and inner diameter 25 mm.The cross section of the ring sample is 2×2 mm.

2.2. Instruments

A special device was built, which can be attached to the X-ray scattering analyzing system Rigaku Denki model-200PL. A line source, with Ni-filtered Cu-Kα, wave length 1.5418Å, was used. The device can stretch and retract the

Table 2
Recipe of compounds

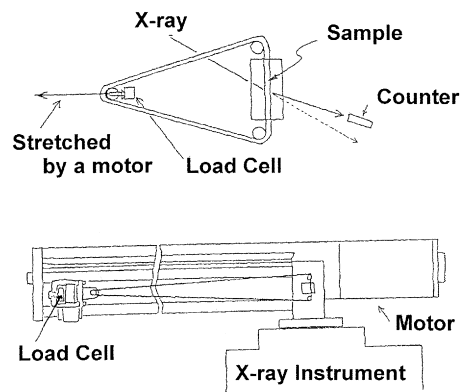| Polymer	100
Stearic-acid	2
N-phenyl-N-isopropyl-p-phenylennediamine	1
ZnO	3
Anti oxidant	1.1
Sulfur	1.5

Fig. 1. Instrument design for simultaneous stress –strain and wide angle X-ray scattering intensity measurement.

sample at constant speed (50 mm/min) and can measure the tensile stress by a built-in load cell. The design of the device is shown in Fig. 1.

2.3. Procedure

Three types of experiments were performed; (i) sequential and (ii) simultaneous stress–strain measurements with wide angle X-ray analysis, and (iii) temperature dependence of the stress–strain relation.

In a sequential measurement procedure, the sample was stretched up to 100% with a stretching rate of 50 mm/min, then stretching was stopped and the wide angle X-ray diffraction pattern was measured. The latter measurement took 30 min to complete. Then the same sample was stretched to 200%, followed by measurement of the wide-angle diffraction pattern, etc.

Simultaneous experiments were performed at 25°C by the newly designed apparatus that allowed the detection of equatorial planes during the stretching. The samples were stretched to desired strains at 50 mm/min until the desired strain is achieved. The stress–strain curves and the X-ray scattering intensity at a given angle-strain relations were recorded by a two-pen $X–Y$ recorder.

The temperature dependence of the strain–stress relations was measured by stretching the sample with a Toyo Baldwin Tensilon testing machine with 50 mm/min speed at desired temperatures.

3. Results and discussion

3.1. Experimental results

Wide-angle X-ray diffraction patterns were measured at 100, 200, and 400% using the sequential procedure described above. In this process the sample was stretched to the desired strains and subsequently taken to the WAXS diffractometer and scanned. This scanning took about 30 min. In these WAXS profiles a peak was observed at 21 degree as shown in Fig. 2. This angle closely corresponds
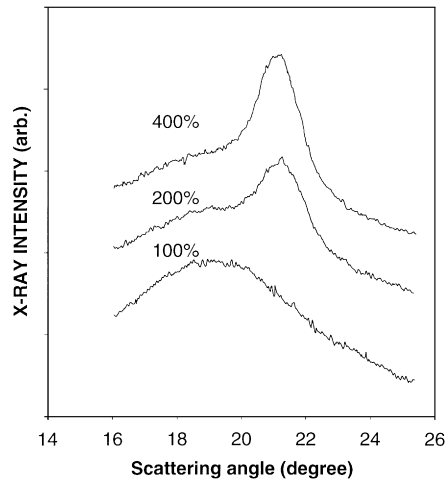
Fig. 2. WAXS diffractometer scans for natural rubber stretched to different deformation levels at 25°C.

to the diffraction angle (21.67 degree) of the (120) plane of the unit cell of natural rubber crystal [16]. The sequential manner of measurements revealed that strain-induced crystallization occurred above 200% strain. This result coincides with the previously reported experiments utilizing sequential measurement procedures.

In order to clarify the dynamics of strain-induced crystallization, we set the goniometer at the (120) peak position and detected the changes of this intensity as a function of strain. The intensity of the scattered X-ray was not normalized for the thickness because the thickness of the sample is not precisely known at a given strain. The degree of crystallinity can be expressed relatively as the height of the scattering intensity at this angle. The simultaneous and
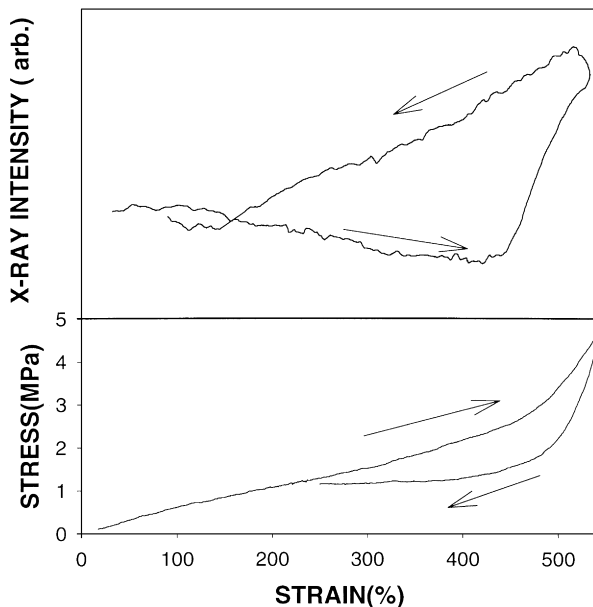

Fig. 3. The stress–strain and X-ray scattering intensity–strain behaviors of natural rubber during stretching and retraction at 25°C.

continuous data of the stress and the intensity of the scattered X-ray during stretching and retraction are shown in Fig. 3. The X-ray intensity goes down until the strain reaches around 400%, then increases steeply. The intensity decrease comes from the decrease of the thickness of the sample, which decreases the total scattering volume of the sample. The average thickness can be calculated at a given strain assuming no volume change during stretching. The scattering body at the given deformation can be converted to the original body volume. The intensity at 0% strain comes from amorphous diffraction of the original scattering body. The apparent crystallization can be calculated by the equation below, derived assuming affine deformation.

$$C_a(x) = I(x)^*(x + 100)^{1/2}/10 - I(0)$$

$C_a(x)$: apparent crystallization at x% strain
$I(x)$: X-ray intensity at x% strain
$I(0)$: X-ray intensity at 0% strain

The apparent crystallization increase was steeper with strain than the X-ray intensity, as shown in Fig. 4. However, it is better to know the behavior of relative intensity with strain than to calculate the value of apparent crystallization, since the true crystallinity can not be determined at a specific scattering angle. Therefore raw intensity data are presented in the remainder of this paper.

Simultaneous measurement does not show any clear intensity increase due to crystallization below 400%. Above 400%, this measurement shows a very steep increase due to crystallization. On the other hand, sequential measurements have shown crystallization to occur at 200% and thereafter to increase gradually. The discrepancy may come from dynamic deformation and equilibrium state of samples. Nishi and Chikaraishi [19] pointed out the possibility of this over-estimation of the crystallinity of natural rubber by a sequential WAXS measurement, comparing with pulsed NMR results.

When the sample is allowed to retract (the strain is decreased) after the sample is stretched to a maximum strain, the stress decreases drastically but the degree of the strain-induced crystallinity still increases for a small degree of decreased strain, then begins to decrease as shown in Fig. 3. The stress during retraction is much lower than the one during stretching. The degree of crystallinity during retraction is higher than that during stretching. Simultaneous birefringence measurements [1,13,15] have shown that the birefringence during retraction is higher than during stretching, but has not shown an increase during retraction. This difference may be due to the fact that the birefringence represents a measure of total orientation of amorphous and crystalline chains. The stress decreases during retraction and starts following the curve as measured during stretching around 200% strain in Fig. 3. The X-ray intensity decreases during retracting and reaches to the level of no crystal scattering intensity during stretching at around 200% also in Fig. 3.

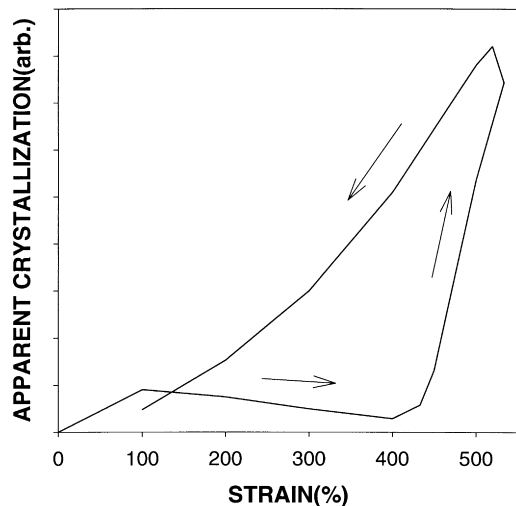When the sample was kept at the maximum strain, stress

Fig. 4. Apparent crystallization-strain behavior of natural rubber during stretching and retraction at 25°C.

Fig. 6. The stress–strain and X-ray scattering intensity–strain behavior of natural rubber during stretching and during retraction to an intermediate strain at 25°C; the temperature of the surrounding was then increased to 80°C.

relaxation occurred and the strain-induced crystallization increased with time as shown in Fig. 5. This increase of degree of crystallization does not depend on strain but does depend on time. These induced crystallites must be different from the crystallites which were developed during stretching.

When the sample was kept at an intermediate strain level in the retraction stage and the temperature of the surrounding was increased by hot air, the stress increased and the degree of the crystallinity decreased with increasing temperature, as shown in Fig. 6. The increase of stress with temperature follows from rubber elasticity, and the decrease in crystallinity comes from a melting of
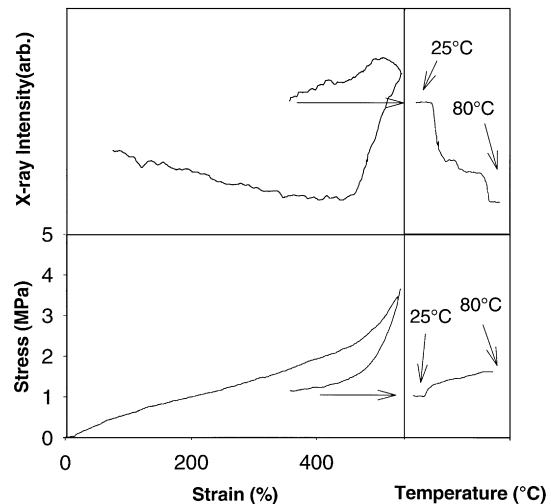
crystallites. Comparisons of the strain-induced crystallization and the stress–strain relations among natural rubber, JSR IR-2200 and Shell Cariflex-309 are shown in Fig. 7. The relations between stress–strain behavior and strain-induced crystallization of the three polymers are very similar. The closure point of the stress–strain loop is almost at the same strain as the closure point of the stress-induced crystallization-strain loop, as shown by the arrows in Fig. 7. The closure point can be considered as the end of melting of the induced crystallinity.

The hysteresis loops of the stress–strain relations at −3, 7 and 22°C measured using a Toyo Baldwin Tensilon tester,
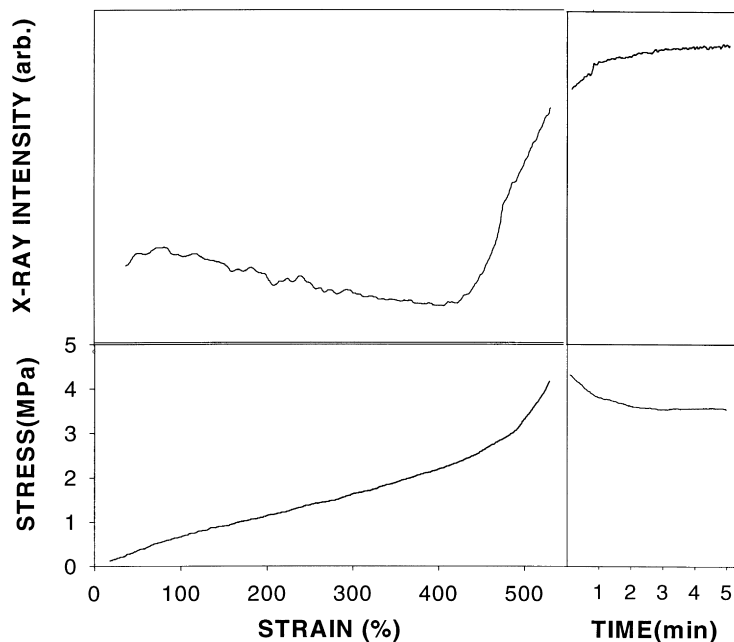

Fig. 5. The stress–strain and X-ray scattering intensity–strain behavior of natural rubber during stretching and after being kept at the maximum strain at 25°C.
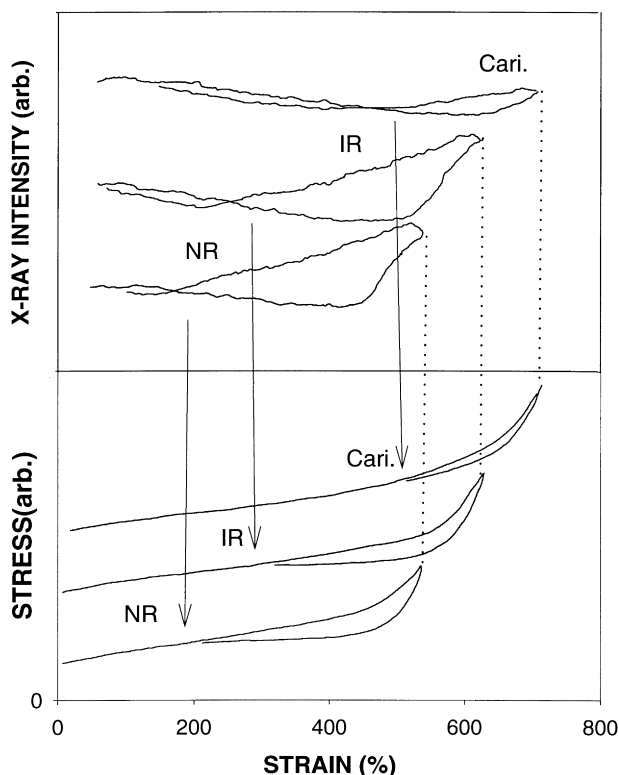
Fig. 7. Comparison of stress–strain and X-ray scattering intensity–strain behaviors of natural rubber, JSR IR-2000 and Shell Cariflex 309 at 25°C.

are shown in Fig. 8. At strains of 0 to 350%, stress–strain relations at these three temperatures are almost the same on this scale of stress, since the increase in stress with temperature for pure natural rubber is small. Around 400%, the −3°C curve shows a clear decrease of stress, whereas the
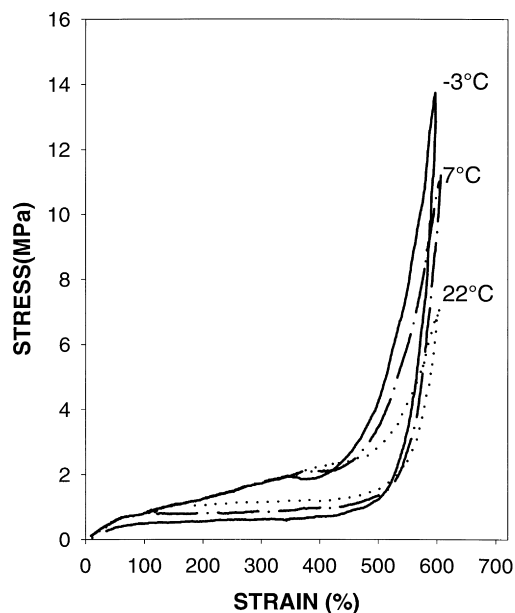

Fig. 8. The hysteresis loop of the stress–strain relation of natural rubber at −3, 7 and 22°C.

22°C curve does not show this decrease. This large difference in stress behavior might be caused by the different amount of extended crystallites formed at these temperatures. Above 450%, the −3°C curve is the first to show a significant steep increase of stress, while the 22°C curve starts its increase last. During retraction, the −3°C curve shows the steepest decrease and the lowest stress in the whole retracting strain region. This suggests that the −3°C condition creates the largest concentration of induced crystallites during retracting. These crystallites do not contribute to the stress and the strain in the crystallites remains near zero strain. At 22°C, the stress–strain loop closes around 200%. The crystallites that were created at 22°C disappeared also at around 200%.

3.2. Discussion

The results of simultaneous measurements suggest two types of strain-induced crystallites that have different dependencies on strain, temperature and time. Several researchers have already pointed out the possibility of a few types of strain-induced crystallites of natural rubber through sequential experiments. Gent [3] suggested a general transformation from polyhedral to aciform (one dimensional) crystallization with strain. Andrews [5–7,20] proposed a schematic diagram illustrating the effect of strain on induced-crystallization, spherulites develop at 0–50% strain levels, row-nucleated shish-kebabs at 100–200%, extended-chain crystals at beyond 400%. Luch and Yeh [8–10] proposed a model that represents the transformation of fibrillar to folded lamella morphology at high elongation.

The real time simultaneous measurement of the stress–strain relation and the strain-induced crystallization can be considered in several stages, as diagrammed in Fig. 9, with proposed molecular models in Fig. 10.

3.2.1. O–A

The stress increases in accordance with rubber elasticity. Orientation of molecular chains has occurred, but strain-induced crystallization is not observed by real time simultaneous measurements. The strain-induced crystallization starts around 400% at 25°C, and around 350% at −3°C, respectively. The extended-chain crystallization first contributes to a decrease in the stress as shown in Fig. 8, since the portion of the chain which is not crystallized behaves as a non-Gaussian chain with a now shorter end-to-end distance as described as A and A′ in Fig. 10. Stage A describes the stretching and orientation of non-Gaussian chains. In stage A′, the chain structure is composed of strain-induced crystallized region and a section whose end-to-end distance is shorter than the un-crystallized non-Gaussian chain. This critical portion of the chain shows lower stress. Actually, the strain continues to increase, the stress decrease being observed only at low temperatures such as −3°C. Flory [21] pointed out this mechanism, that is, crystallization should lower the stress levels.
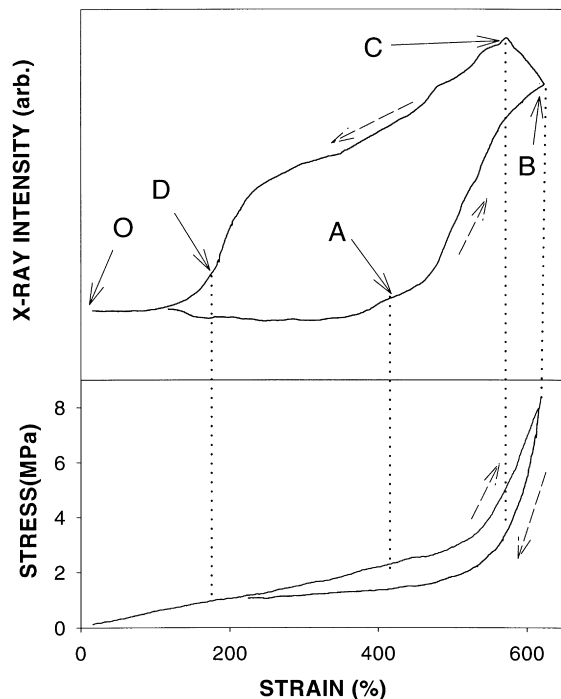
Fig. 9. The relationship of stress–strain behavior for a series of stages during stretching and retraction.

3.2.2. A–B

The stress increases drastically with strain-induced crystallization. The stress at around 550% might be born by the energetic (no entropy) modulus of extended chain crystals. According to the stress relaxation experiments at point "B", the crystallinity increases with time, without increase of strain. This result suggests that secondary crystallites develop with time at high strain. Andrews [5–7] suggested the lamellar growth would lead to a reduction of stress by his thin film experiment. Luch and

Yeh [8–10] pointed out that stress relaxation is a direct consequence of lamella formation in highly stretched natural rubber at low temperature. At high deformation, network points would move to relax the stress of some network chains. Then these relaxed chains would form folded lamellae at the surface of extended-chain crystal.

3.2.3. B–C

The stress decreases steeply and shows much lower value than that during stretching. The strain-induced crystallinity increases a little or at least there is no drastic change. The value of crystallinity during retracting shows a much higher value than that during stretching. This tendency coincides with the simultaneous birefringence result [1,13,15]. The whole orientation does not change significantly, although the stress decreases drastically. Strain-induced crystallites might transform their morphology to secondary crystallites that do not contribute to the stress. Secondary crystallites might be the same morphology as the ones causing the stress relaxation at point "B". The morphology model proposed in stage C is shown in Fig. 10.

3.2.4. C–D

The stress is lower than that during stretching. But the crystallinity and orientation are larger than that during stretching. This result suggests that the number of non-Gaussian network chains that are able to bear stress is reduced significantly, possibly due to secondary crystallization. The total concentration of strain-induced crystallites decreases with the retracting strain. At point "D", the strain-induced crystallites have disappeared. The stress during stretching and the stress during retraction coincide. The strain-induced crystallites are totally melted at strain "D". Below point "D", the stress–strain curves during stretching and retracting follow the same line.

3.3. Model

The crystallites formed by deformation may be composed of two types:

Type 1. The main portion of crystallites are extended-chain crystallites that develop by the strain directly during stretching. During retraction, most of this type of crystallites transforms rapidly to the secondary lamella crystallites.
Type 2. The secondary crystallites might be folded-chain lamellae. These develop during retraction and decrease in concentration with decreasing strain. Without a further increase of strain, this type of crystallite is able to form at low temperature.

The hysteresis of the stress–strain relation is attributed to the formation of the stress induced crystallites and their transformation.
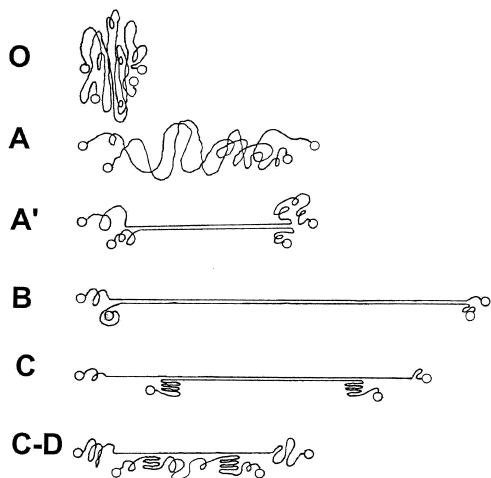

Fig. 10. A model depicting strain-induced crystallization mechanism of NR. The open circle indicates cross-link points. The lines are network chains. See text for discussion of O–A, A′, B–C and C–D.

Real-time simultaneous measurements reveal that the dynamics of these two types of strain-induced crystallites is important to the stress–strain behavior of natural rubber.

4. Conclusions

Real-time simultaneous measurements disclose the dynamics of strain-induced crystallization. These results differ from the results of sequential measurements. During stretching, molecular chains show orientation, but no crystallization takes place until around 400% at 25°C. Above 400%, strain-induced crystallization occurs and increases steeply. At the strain at which retraction starts, most of the strain-induced crystallites appear to change to the secondary strain-induced crystallites that do not contribute to stress. The crystallinity decreases with decreasing strain, and the crystallites completely melt at the strain at which the stress–strain loop closes. Therefore the hysteresis of the stress–strain relation is attributed to strain-induced crystallization and their transformation.

Acknowledgements

References

[1] Treloar RG. The physics of rubber elasticity, 3rd ed. Oxford: Oxford University Press, 1975.
[2] Flory PJ. J Chem Phys 1947;15:397.
[3] Gent AN. Trans Faraday Soc 1954;50:521.
[4] Smith Jr. KJ, Greene A, Ciferri A, Kolloid-Z uZ. Polymere 1963;194:49.
[5] Andrews EH. Proc R Soc 1962;A270:232.
[6] Andrews EH. Proc R Soc 1964;A272:562.
[7] Andrews EH, Owen PJ, Singh A. Proc R Soc Lond 1971;A324:79.
[8] Luch D, Yeh GSY. J Appl Phys 1972;43:4326.
[9] Luch D, Yeh GSY. J Macromol Sci Phys 1973;B97:121.
[10] Luch D, Yeh GSY. J Polym Sci Polym Phys 1973;11:467.
[11] Edwards BC, Phillips PJ. J Polym Sci Polym Phys 1975;13:2117.
[12] Edwards BC, Phillips PJ, Sorensen D. J Polym Sci Polym Phys 1980;18:1737.
[13] Mukherjee DP. Rubber Chem Technol 1974;47:1234.
[14] Hashiyama M, Gaylord R, Stein S. Die Makromo Chem Suppl 1975;1:579.
[15] Suzuki A, Oikawa H, Murakami K. J Macromol Sci Phys 1985;B23:535.
[16] Shimomura Y, White JL, Spruiell JE. J Appl Polym Sci 1982;27:3553.
[17] Siesler HW. Applied Spectroscopy 1985;39:761.
[18] Mitchell GR. Polymer 1984;25:1562.
[19] Nishi T, Chikaraishi T. J Maromol Sci Phys 1981;B19(3):445.
[20] Phillips PJ. Rep Prog Phys 1990;53:549.
[21] Flory PJ. Principles of polymer chemistry, Cornell: Cornell University Press, 1953.